HHS Public Access

Author manuscript

Immunol Invest. Author manuscript; available in PMC 2021 January 20.

Published in final edited form as:

Immunol Invest. 2020 October ; 49(7): 744–757. doi:10.1080/08820139.2020.1803353.

An Immunosuppressive effect of Melanoma-derived Exosomes on NY-ESO-1 antigen-specific human CD8+ T cells is dependent on IL-10 and independent of BRAF^{V600E} mutation in melanoma cell lines

Shin La Shu[*,a], **Junko Matsuzaki**[b], **Muzamil Y. Want**[b], **Alexis Conway**[c], **Shawna Benjamin-Davalos**[a], **Cheryl L. Allen**[a], **Marina Koroleva**[a], **Sebastiano Battaglia**[b], **Adekunle Odunsi**[b], **Hans Minderman**[c], **Marc S. Ernstoff**[a]

[a]Department of Medicine, Roswell Park Comprehensive Cancer Center, Buffalo, NY

[b]Center for Immunotherapy, Roswell Park Comprehensive Cancer Center, Buffalo, NY

[c]Flow and Image Cytometry Shared Resource, Roswell Park Comprehensive Cancer Center, Buffalo, NY

Abstract

Exosomes, including human melanoma-derived exosomes (HMEX), are known to suppress the function of immune effector cells, which for HMEX has been associated with the surface presence of the immune checkpoint ligand PD-L1. This study investigated the relationship between the BRAF mutational status of melanoma cells and the inhibition of secreted HMEX exosomes on antigen-specific human T cells. Exosomes were isolated from two melanoma cell lines, 2183-Her4 and 888-mel, which are genetically wild-type BRAF^{WT} and BRAF^{V600E}, respectively. HMEX were isolated using a modified, size-exclusion chromatography (SEC) method shown to reduce co-isolation of non-exosome associated cytokines compared to ultracentrifugation isolation. The immunoinhibitory effect of the exosomes were tested in vitro on patient-derived NY-ESO-1-specific CD8$^+$ T cells challenged with NY-ESO-1 antigen. HMEX from both cell lines inhibited the immune response of antigen-specific T cells comparably, as evidenced by the reduction of IFN-γ and TNF-α in NY-ESO-1 tetramer positive cells. This inhibition could be partially reversed by the presence of anti-PD-L1 and anti-IL-10 antibodies. IL-10 has been demonstrated to be a critical pathway for sustaining enhanced tumorigenesis in BRAF^{V600E} mutant cells compared to BRAF^{WT} melanoma cells. Thus, we demonstrate that HMEX inhibit antigen-specific T cell responses independent of the BRAF mutational status of the parent cells. In addition, PD-L1 and IL-10 contribute to the HMEX mediated immune-inhibitory activity of antigen specific human T cells. The inhibitory capacity of exosomes should be taken into consideration when developing therapies that are reliant upon the potency of customized, antigen-specific effector T cells.

[*]Corresponding author: Shin La Shu, Affiliate Member, Department of Medicine, Roswell Park Comprehensive Cancer Center, 665 Elm St, Buffalo, NY 14203, shinla.shu@RoswellPark.org.

Declaration of interest statement

All authors (S.S., J.M., M.Y.W., A.C., S.B., C.L.A., M.K., S.B., A.O., H.M., and M.S.E) declare no potential conflict of interest.

Keywords

NY-ESO-1; T cells; exosomes; IL-10; PD-L1; immunosuppression

Introduction

Cancer-derived cytokines and extracellular vesicles (EVs) contribute to the tumor niche as well as the pre-metastatic niche in more distal noncancerous environments (Shu et al. 2018; Whipple et al. 2016). Consequently, cancers like melanoma are particularly predisposed to poor outcomes due to metastasis as more than 95% of patients die from metastatic burden without intervention. Genetically distinct melanomas will often display varied biological behavior (Ellerhorst et al. 2011; Ilieva et al. 2014).

Amongst EVs secreted by melanoma, a subset of EVs ranging in size from 50 to 120 nm in diameter are capable of directly influencing stromal cells to promote the generation of pro-tumor conditions within the tumor microenvironment (TME). More commonly known as exosomes, these vesicles contain nucleic acid and protein cargo, and are decorated with membrane molecules. Exosomes are released by specific endosomes called multivesicular bodies (MVBs) into the extracellular environment (Russell et al. 2019). Secreted HMEX can fuse with local stromal cells, where they promote metabolic reprogramming and can also influence distal sites via the bloodstream or lymphatic action (Ilieva et al. 2014; Tung et al. 2019).

Melanoma cells produce soluble factors such as cytokines which can regulate cells in the TME. For example, cytokine synthesis inhibitory factor IL-10 promotes immunosuppression by suppressing expression of ILs-1a, 1b, −6, −12 and −18, TNF-α and GMCSF in T cells and macrophages, as well as IFN-γ in activated T-helper cells. IL-10 has been demonstrated to be a critical pathway for sustaining enhanced tumorigenesis in BRAF V600E mutant cells compared to WT BRAF melanoma cells (Ascierto et al. 2012; Khalili et al. 2012). HMEX membranes are decorated with molecules such as Programmed death-ligand 1 (PD-L1) that directly suppresses the anti-tumor activity of T cells. Recently, exosomal PD-L1 has been identified as an underlying cause of T cell suppression and as a biomarker of poor prognostic outcome (Chen et al. 2018). Tumor derived exosomes are also potent inhibitors of other immune cells such as DCs, NK T cells and neutrophils (Whiteside 2016, 2018; Sharma et al. 2020).

To better understand the contribution of exosome mediated pathways and tumor derived soluble factors which may co-isolate with exosomes, we employ ultrafiltration columns coupled with size exclusion chromatography (SEC) columns which increase the yield and purity of HMEX compared to isolating exosomes by ultracentrifugation methods (Shu et al. 2020).

The current study demonstrates that exosome-associated IL-10 and PD-L1 are involved in the HMEX immuno-suppressive effects on tumor antigen-specific T cells, independent of the BRAF status of the primary melanoma cell line.

Materials and Methods

Cell culture of melanoma cell lines for HMEX isolation

Melanoma cell lines 2183-Her4 ($BRAF^{WT}$) and 888-mel ($BRAF^{V600E}$) were obtained from National Institutes of Health (NIH). The cell lines were checked for mycoplasma regularly and were mycoplasma free during the conduct of the presented studies. Chinese Hamster Ovary (CHO) cells and HL-60 wild-type (HL60wt) cells were kindly provided by Dr. Hans Minderman (Roswell Park Comprehensive Cancer Center). Mel624.38 were kindly provided by Dr. Kunle Odunsi, as well as obtained from NIH. Validation of cell line authenticity was performed by the Genomic Shared Resource (Roswell Park Comprehensive Cancer Center) using short tandem repeat analysis (STR DNA fingerprinting). Cells were maintained in RPMI 1640 media supplemented with GlutaMAX (Gibco, USA), Penicillin/Streptomycin (Gibco, USA) and 5% fetal bovine serum (FBS, Gibco, USA). Twenty-four hours before harvesting supernatants for HMEX, adherent cells were washed with “supplement-free” RPMI 1640 media and then cultured with exosome-depleted complete media which contains 5% exosome-depleted FBS (Gibco, USA).

Isolation of exosomes from melanoma cells lines

Exosomes were isolated as described previously (Shu et al. 2018) using the REIUS (Rapid Exosome Isolation Using Size exclusion chromatography) method. In brief, cell culture supernatant was centrifuged at 300 × *g* for 5 minutes to pellet cells. The resultant supernatant was decanted into a 50 ml Falcon tube for centrifugation at 3000 × *g* for 15 minutes for removal of cell debris. The supernatant was transferred to a new 50 ml Falcon tube and passed through a 0.20 μm PES syringe filter (FisherScientific, USA) to eliminate contaminating particles greater than 200 nm in size. The filtered supernatant was transferred to Amicon Ultra-15 Centrifugal Filter Units, MWCO 100 kDa (Millipore Sigma, USA), and spun down to an appropriate volume for use in Exo-spin SEC columns in accordance with manufacturer’s instructions (Cell Guidance Systems, USA).

Exosome size and concentration measurements by NTA

Size and concentration of purified exosomes were determined by nanoparticle tracking analysis (NTA) using ZetaView (Particle Metrix, USA) equipped with a 405 nm light source. Samples were run at 25°C using 0.20 μm-filtered PBS as a diluent. For video acquisition, a shutter speed of 600 and frame rate of 60 were used; sensitivity was set at 89 in accordance with software guidance algorithms. Prior to taking measurements, particle detection accuracy was verified using 100 nm non-labeled latex beads (Applied Microspheres, The Netherlands). For fluorescence NTA, detection accuracy was verified using 100 nm yellow-green microspheres (Polysciences Inc, USA) with a 650 nm long pass filter in the emission path. Samples were diluted in PBS to achieve a particle count in the range of 200–500. Isolated HMEX were analyzed by non-fluorescent (excitation 405 nm, no emission filter) and fluorescent NTA (405 nm excitation, 650 nm long-pass emission filter) modes. The fluorescent NTA performance was validated using 100 nm Fluorescent beads by determining no statistically significant differences in size and concentration measurements of the fluorescent bead suspension both in non-fluorescent (mean size ± SD of 127.2 ± 54.7 nm,

18×10^{13} particles/ml) and fluorescent mode (mean size 107.3 ± 30.2 nm, 5.7×10^{13} particles/ml).

Conjugation of PD-L1 antibody with quantum dot (Qdot) 705

PD-L1 antibody clone MIH1 (Thermo Scientific, USA) was conjugated with Qdot 705 using the ThermoFisher (S10454) SiteClick Antibody Labeling Kit (Qdot 705) according to the manufacturer's instructions. The resulting conjugated antibody was subsequently purified using the Abcam Mouse Antibody Purification Kit (ab128745), according to manufacturer's instructions.

Imaging Flow Cytometry

Labeled HMEX were acquired using an imaging flow cytometer ImageStream MK-II (Millipore, USA). About 5,000 individual images were recorded; spectral compensation and analyses were performed using ImageStream Data Exploration Software. Unlike fluorescent NTA which necessitated the need for the PD-L1 antibody to be conjugated to photostable Qdot 705 (see results section), the shorter excitation of the fluorochromes during imaging flow cytometry does not present a problem with regards to photobleaching. Therefore, an anti-PD-L1 antibody directly conjugated to Brilliant violet 421 (BV421; BD, USA) could be used. The antibody was clone-matched with the antibody used during fluorescent NTA and used at a dilution factor of 1:100. For an antibody control, BV421 antihuman-PD-L1 antibody was diluted 1:100, without the addition of exosomes. To determine which population in the image corresponded to exosomes, the test sample was then lysed with 0.5% Triton-X prepared in 1X PBS, mixed by inverting the tube several times over the course of 10 minutes and re-analyzed by ImageStream for the loss of any specific population.

NY-ESO-1-specific $CD8^+$ T cell isolation

HLA-A2-restricted NY-ESO-1-specific $CD8^+$ T cells were isolated from peripheral blood of a testicular cancer patient who had anti-NY-ESO-1 antibody response as described previously (Matsuzaki et al. 2015; Matsuzaki et al. 2010). Briefly $CD8^+$ T cells were separated using magnetic beads (Invitrogen) followed by stimulation with NY-ESO-1 pooled peptide-pulsed autologous $CD4^-CD8^-$ cells. HLA-A2/NY-ESO-$1_{157–165}$ tetramer$^+CD8^+$ T cells were sorted by FACSAria (BD Biosicences) and expanded by stimulation with phytohemaglutinin (PHA, Thermo Scientific) in the presence of γ-irradiated normal donor PBMC, IL-2 (Sigma) and IL-7 (R&D Systems).

Exosome co-culture with T cells / neutralizing antibody and analysis by flow cytometry

HLA-A2-resticted NY-ESO-1-specific $CD8^+$ T cells ($5–10\times10^4$) were co-cultured with 6×10^{10} HMEX per well for 48 h in the presence of 10U/ml IL-2 and 10 ng/ml IL-7 in RPMI 1640 media supplemented with 5% exosome-depleted FBS. Neutralizing antibody (monoclonal) for human PD-L1 was purchased from Thermo Scientific and was present at a neutralizing concentration of 5 μg/ml based on previous studies (Matsuzaki et al. 2015). Neutralizing antibody for human IL-10 (monoclonal) was purchased from R&D systems, and was present at a neutralizing concentration in accordance to manufacturer's

recommended concentration (i.e. 2 μg/ml, which would neutralize > 60% of the bioactivity due to 5 ng/ml of IL-10). HMEX were pre-incubated for 18 hours with PD-L1 and IL-10 neutralizing antibodies, separately or in combination, prior to incubating with the T cells. After the incubation, T cells were washed with media and incubated with HLA-A2$^+$NY-ESO-1$^+$ Mel624.38 cells for 4 h in the presence of 5 μg/ml of monensin (Sigma). Thereafter, cells were stained with HLA-A2/NY-ESO-1$_{157–165}$ tetramer (MBL) and CD8 (BioLegend), fixed with 2% formaldehyde and permeabilized to stain intracellular IFN-γ (BD Biosciences) and TNF-α (BD Biosciences) as described previously (Matsuzaki et al. 2015). The cells were analyzed using a BD LSR Fortessa cell analyzer and % cytokine production on tetramer$^+$CD8$^+$ T cells was analyzed by FlowJo software. PD-1 surface expression was examined using flow cytometry after staining T cells with APC conjugated PD-1 antibody (Biolegend) or its matched isotype control (Biolegend). PD-1 expression was quantified by comparing the specific PD-1 intensity distribution with the matched isotype control using the Kolmogorov-Smirnov (KS) statistic D-value (WinList version 9.0.1, Verity Software House)

Cell viability and detection of apoptosis

For calculation of cell viability, cell number was counted using a Bio-Rad TC20 automated cell counter with trypan blue exclusion (Bio-Rad, USA). For the detection of apoptosis, a FITC Annexin V Apoptosis Detection Kit I (BD, USA) was used in accordance to the manufacturer's protocol.

Statistical analysis

Statistical analysis was performed with GraphPad Prism 8.3.0 by GraphPad Software Inc. (San Diego, CA). ANOVA was used to determine *p*-value, with a *p*-value less than 0.05 being statistically significant. Experiments were done in triplicate. Error bars represent mean ± SE (standard error of the means). Number of asterisks denote increasing statistical significance (* implies *p*-value < 0.05, ** < 0.01, *** < 0.005 and **** is < 0.001). Kolmogorov-Smirnov statistic (KS statistic) was used to compare the cumulative distributions between positive signals in PD-1 isotype control and PD-1 antibody samples. Test statistic (D-values) were calculated by subtracting isotype control histograms from the PD-1 specific histograms using the Winlist version 9.0.1 software.

Results

Fluorescent NTA detects less than 1% of HMEX to be PD-L1 positive

The application of fluorescence NTA is limited by the photostability of the fluorescent probes. NTA uses laser-derived scatter of small particles to record their Brownian motion. In order to record sufficient particle trace-lengths for accurate determination of particle size, particles are subjected to laser excitation for relatively long periods versus flow cytometry. Therefore, the most commonly used flow cytometry fluorochromes are not suitable for fluorescence NTA due to premature photobleaching. Attempts to quantify HMEX expressing PD-L1 using Alexa Fluor 488 or 647 conjugated antibodies failed due to photobleaching (data not shown). To overcome this limitation, the PD-L1 antibody was conjugated to Qdot 705 using commercial kits for conjugation and antibody purification, as quantum dots are

highly photostable semi-conductive nanoscale crystals. The performance of the Qdot 705-PD-L1 antibody was compared with a CHO cell line with known expression of PD-L1 (Fig 1A).

Validation of fluorescent NTA was conducted by detecting particles of the same size and concentration in both fluorescent and non-fluorescent NTA using 100 nm fluorescent beads in suspension. Unstained HMEX were determined to have a mean size of 91 nm which increased to 151 nm after the addition of the Qdot 705-PD-L1 antibody (Fig 1B). The increase in size of stained HMEX can be attributed to the presence of the Qdots that range in size from 15–21 nm. Less than 1% of particles detected in non-fluorescent NTA (concentration: 2.8×10^{10} /ml) were detected in the fluorescent NTA mode (concentration: 9.0×10^{7} /ml) which may indicate that PD-L1 positive EVs are less than 1% of all exosomes isolated using the REIUS method.

Imaging flow cytometry validates the PD-L1 positive HMEX population to be sensitive to detergent lysis

A commercial anti-PD-L1 antibody directly conjugated to BV421 (same clone) was used to label HMEX for flow cytometry analysis. While absent in the antibody-only control sample (Fig 1C), a population of PD-L1 positive particles was detected when analyzing HMEX + α-PD-L1 (Fig 1D). Furthermore, this population was not present upon the addition of the detergent Triton-X to antibody-treated HMEX (Fig 1E). Taken together, this provides evidence that although they are a small population among exosomes (<1%), PD-L1 positive exosomes can be detected by both fluorescent NTA and flow cytometry methods.

HMEX display immunosuppressive effects on antigen-specific T cells irrespective of BRAF mutation status of parent cells

NY-ESO-1 is a tumor antigen expressed in melanoma, breast, prostate, thyroid and ovarian tumors, and is not expressed in normal adult tissues except the testes. To test the immunosuppressive effects of HMEX on antigen-specific T cells, patient derived NY-ESO-1 tetramer positive $CD8^+$ T cells (NY-T cells) were challenged in vitro by exposure to HLA-$A2^+$ Mel 624.38 melanoma cells that express NY-ESO-1 (Matsuzaki et al. 2015; Matsuzaki et al. 2010). Immune function was assessed by intracellular production of IFN-γ and TNF-α while the identity of the antigen-specific T cells was determined through binding of an NY-ESO-1-specific tetramer. Approximately 92 – 95% of the NY-T cells were tetramer positive (Fig 2A). In the absence of HMEX, coincubation of NY-T cells and Mel 624.38 cells for 24 hours caused 65.9% of tetramer positive NY-T cells to produce IFN-γ and 23.0% to produce TNF-α (Fig 2B). However, the percentage of IFN-γ-producing NY-T cells decreased to 30.8% when cultured in the presence of 888-mel HMEX and to 34.6% in the presence of 2183-Her4 HMEX, while TNF-α-producing NY-T cells was reduced to 13.6% and 14.3% in the presence of 888-mel HMEX and 2183-Her4 HMEX, respectively (Fig 2B). Thus, the percentage of IFN-γ and TNF-α producing NY-T cells was reduced by more than 50% when cultured in the presence of HMEX, regardless of the BRAF mutational status of the HMEX cells of origin. To address whether the observed immunosuppression could be attributed to loss of T cell viability due to exosomes (Zhang and Grizzle 2011), Annexin V/Propidium Iodide analysis was performed. No noticeable change in the apoptotic fraction or

loss in viability in T cells were observed when HMEX was were co-cultured with T cells (Supplementary Fig 1).

Dual inhibition of PD-L1 and IL-10 necessary to revert immunosuppressive effects of HMEX exosomes on NY-T cells

In our previous work, we showed that both 888-mel and 2183-Her4 HMEX express PD-L1 (Shu et al. 2020), so we hypothesized that the presence of PD-L1 positive HMEX may be partially responsible for the inhibition of IFN-γ and TNF-α seen in NY-T cells. Interestingly, we found that the inhibition of PD-L1 using neutralizing antibodies does not rescue the number of cells producing IFN-γ or TNF-α to levels seen upon incubation of NY-T cells with Mel624.38 cells alone (Figs 3A–E). Another pathway shown to promote suppression of antigen-specific T cell activity is the IL-10 inhibitory pathway (Brooks et al. 2008) and previous studies have demonstrated that IL-10 is significantly produced in BRAF V600E mutant melanoma cells (Sumimoto et al. 2006). Interestingly, when 888-mel or 2183-Her4 HMEX were treated with anti-IL-10 antibodies for 18h prior to incubation with NY-T cells, we saw little to no increase in the percentages of IFN-γ or TNFα producing NY-T cells compared to NY-T cells incubated with HMEX alone (Figs 3B–E; Supplementary Fig 2). To investigate this further, NY-T cells were co-incubated with HMEX neutralized with both anti-PD-L1 and anti-IL-10. Here we found that blocking both PD-L1 and IL-10 was necessary to revert the immunosuppressive effect seen in NY-T cells upon incubation with both 888-mel and 2183-Her4 HMEX. However, though there was only a partial rescue in IFN-γ producing NY-T cells treated with PD-L1 and IL-10 neutralized 888-mel HMEX, the percentage did increase from 31% to 56% when compared to incubation with non-neutralized HMEX. Thus, our data suggests that collectively, exosomal PD-L1 and IL-10 are capable of significantly reducing IFN-γ and TNF-α positive NY-T cell populations that can be partially reversed with PD-L1 and IL-10 neutralizing antibodies. This study corroborates another published report showing that the blockade of the IL-10 receptor together with PD-1 (PD-L1 receptor on $CD8^+$ T cells) can synergistically increase functional activity of NY-ESO-1 specific $CD8^+$ T cells (Sun et al. 2015). This finding may have significant implications in reducing anergy of tumor antigen-specific $CD8^+$ T cells observed in immunotherapy of melanoma patients in a clinical setting.

Discussion

Exosomes have been implicated in the modulation of the immune response through expression of immune checkpoint proteins like PD-L1 and other immune modulating proteins found on the exosomal membrane. The proto-oncogene B-Raf (BRAF)-directed mitogen-activated protein kinase (MAPK) pathway may be activated through the $BRAF^{V600E}$ mutation and is a strong driver of cancer-immune evasion predominantly through the PD-L1/PD-1 checkpoint inhibitor pathway (Khalili et al. 2012; Sumimoto et al. 2006; Shabaneh et al. 2018). Moreover, $BRAF^{V600E}$ mutation can directly increase PD-L1 levels on tumor cells (Feng et al. 2019).

Nevertheless, there is a subset of advanced melanoma patients who do not respond to anti-PD-1 antibody therapy irrespective of their $BRAF^{WT}$ or $BRAF^{V600E}$ mutation status (Robert

et al. 2015). Based on our study, we have determined that HMEX derived from either $BRAF^{V600E}$ or $BRAF^{WT}$ cell lines have similar immunosuppressive potency and employ similar pathways. Using fluorescent-NTA, we determined that isolated HMEX contain a very small population of PD-L1 positive exosomes.

For our exosomal PD-L1 study, we used 888-mel $BRAF^{V600E}$ melanoma cell line exosomes for the purpose of direct detection of PD-L1 using NTA and imaging flow cytometry, as 888-mel not only release more exosomes but also have higher PD-L1 positivity than 2183-Her4 exosomes (Shu et al. 2020). The photo-labile properties of commercially available fluorophores conjugated to the PD-L1 specific antibody in NTA applications necessitated custom conjugation to the photostable QDot 705. The specificity of the QDot705 conjugated anti-PD-L1 antibody was not compared to an isotype control since the conjugation efficiency of the commercial conjugation kit used is not known and therefore it would invalidate such a comparison which requires identical fluorochrome:IgG ratios for the specific antibody and its isotype. Validation of specificity of the anti-PDL1 antibody clone is provided in Supplementary Fig 3 (specific staining compared to isotype control in PD-L1+ CHO line and negative staining in PD-L1-HL60wt line).

This study demonstrates that exosomes interfere with the production of IFN-γ and TNF-α, both of which are antitumor cytokines in NY-T cells. Studies have shown that IFN-γ and TNF-α play an important role in immune system surveillance of tumor growth by effectively triggering tumor cell death via activation of the NF–κB, JAK/STAT and MAPK pathways, among others (Mortara et al. 2007; Ikeda, Old, and Schreiber 2002). Therefore, therapeutic strategies reliant upon the infiltration of antigen-specific T cells are vulnerable to the inhibitory influence of exosomes. HMEX from both $BRAF^{V600E}$ and $BRAF^{WT}$ cell lines contain detectable levels of PD-L1 and secrete IL-10, thus we evaluated whether inhibiting PD-L1 alone or in combination with anti-IL-10, could reverse the immunosuppressive effect of HMEX. We found that neutralizing with both PD-L1 and IL-10 antibodies is required to reverse the immunosuppression caused by these exosomes in antigen-specific T cells.

Although the relationship between IL-10 and T cells within the TME is not entirely understood, we are beginning to gain clarity. Previously it was demonstrated that the presence of IL-10 improves T cell activity, however this observation was made in T cells with low tumor cell-specific responses (Mumm et al. 2011; Emmerich et al. 2012). Antigen-specific T cell activity is crucial to understanding tumor surveillance. Such T cells are strongly inhibited by the presence of IL-10 and display synergistic inhibition when coupled with an immune checkpoint-inhibitor pathway such as PD-1 (Sun et al. 2015). We demonstrate that HMEX-associated IL-10 and PD-L1 work synergistically to promote HMEX-induced immunosuppression in NY-T cells. We also examined whether NY-T cells are PD-1 positive at the point of co-incubation with HMEX, but PD-1 levels were slightly positive with a mean KS statistic D-value of 2.75% for the triplicate measurement (Supplementary Fig 4). Since NY-T cells can increase PD-1 level by stimulation with anti-CD3 (Liu et al. 2019), it is possible that PD-1 level may be increased during co-incubation with HMEX and the PD-1/PD-L1 axis is triggered to induce immunosuppression. An important issue relevant to these studies is the activation status of T cells before co-culture with Mel624.38 cells. NY-T cells used in the study are expanded with PHA and cultured in

the presence of IL-2 and IL-7. Since PHA itself is a strong activation stimulus and IL-2 can induce IFN-γ production (Kasahara et al. 1983) and TNF-α (Lorre, Fransen, and Ceuppens 1992) in T cells, while IL-7 can induce TNF-α production (Roato et al. 2006), the cells were cultured for 10 days until spontaneous IFN-γ and TNF-α was no longer detected, before co-incubation with Mel624.38 cells (See Figure 3, PBS: unactivated T cell control).

Partial recovery of IFN-γ and TNF-α- producing T cells upon the blocking of HMEX with anti PD-L1 and IL-10 antibodies may hint at the involvement of other unknown pathways in the inhibitory action of exosomes. Our data indicate that the observed reversal of HMEX-induced activation of T cells by anti-PD-L1 and anti-IL10 antibodies (Fig 3) is HMEX-dependent since a potential independent effect is ruled out by demonstrating that the anti-PD-L1 and IL10 antibodies or their isotypes have no effect on the Mel-induced T-cell activation by themselves. It is possible that the presence of other inhibitory factors such exosomal FasL or TGF-β may cause such suppression, as reported by other groups (Sharma et al. 2020). In addition, lipids such as phosphatidylserine (Kelleher et al. 2015; Keller et al. 2009; Matsumura et al. 2019), ganglioside GD3 that is shed in melanomas and melanoma exosomes (Sa et al. 2009; Shenoy, Loyall, Berenson, et al. 2018) or tumor-derived exosomal RNA are also reported to be immunosuppressive (Maybruck et al. 2017). In contrast to other studies that demonstrated apoptosis and loss of cell viability in T cells when co-cultured with exosomes, we did not observe such a disruption in cellular survival that would cause a loss in T cell activation when the NY-T cells were co-cultured with HMEX isolated using the REIUS method.

A recent report suggested that based on proteomic profiling, EVs from exudative seroma-derived vesicles carrying melanoma-specific signatures and the $BRAF^{V600E}$ mutation correlated with a reduction in disease-free survival (Garcia-Silva et al. 2019). Although our findings demonstrate that isolated HMEX from both $BRAF^{V600E}$ and $BRAF^{WT}$ cell lines are equally immunosuppressive, IL-10 is released in significantly higher quantities by $BRAF^{V600E}$ mutant cell line versus the $BRAF^{WT}$ cell line. Thus, a high concentration of IL-10 may provide an additional layer of immunosuppressive signaling that may continue to cripple potency of tumor antigen-specific $CD8^+$ T cells during PD-L1 blockade intervention therapies. Our data suggests that the greater immunosuppressive ability or aggressiveness of $BRAF^{V600E}$ mutants could be related to increased activation of the IL-10 pathway compared to $BRAF^{WT}$ and hence this could possibly explain differences observed in the immune responses between $BRAF^{V600E}$ and $BRAF^{WT}$ melanomas. This observation strongly supports the role of cancer-derived exosomes in immune suppression and identifies another target for therapy (Marleau et al. 2012). The inhibition of antigen-specific T cell activation by tumor-derived exosomes has been demonstrated previously (Shenoy, Loyall, Maguire, et al. 2018), but to our knowledge the current study is the first to demonstrate tumor antigen specific $CD8^+$ T cells can also be immunosuppressed by tumor-derived exosomes. There are several limitations to this study. Firstly, it does not factor in the possibility of the cytokine IL-10 present within exosomes as cargo, since it is a vesicle and the neutralizing antibodies only binds to accessible IL-10 that is co-isolated with exosomes. Secondly, Mel624.38 cells that are co-incubated with T cells can also release exosomes. However, the short incubation period (4 h) makes it unlikely to be a contributing factor to the study. Caution is also advised when T cell-centric therapies are implemented without consideration of exosomes as an

important factor within the TME. Taken together, exosomal PD-L1 is immunosuppressive and soluble cytokines such as IL-10 can synergistically inhibit antigen-specific T cell IFN-γ and TNF-α production, and therefore should be considered an important factor when T cell suppression is observed in tumor antigen-specific T cell activity.

Supplementary Material

Refer to Web version on PubMed Central for supplementary material.

Acknowledgements

We would like to thank Terence Tan., M.D. for his assistance in editing the manuscript. This work was supported by The Katherine Anne Gioia Endowed Chair in Cancer Medicine, Roswell Park Comprehensive Cancer Center; RPCI-UPCI Ovarian Cancer SPORE P50CA159981-01A1; National Cancer Institute (NCI) grant P30CA016056 involving the use of Roswell Park Comprehensive Cancer Center's Flow and Image Cytometry Shared Resources and Immune Analysis Shared Resource, Roswell Park Alliance Foundation; NIH grants 1R50CA211108 (H.M.) and S10OD018048 (H.M.)

References

Ascierto PA, Kirkwood JM, Grob JJ, Simeone E, Grimaldi AM, Maio M, Palmieri G, Testori A, Marincola FM, and Mozzillo N. 2012 'The role of BRAF V600 mutation in melanoma', J Transl Med, 10: 85. [PubMed: 22554099]

Brooks DG, Ha SJ, Elsaesser H, Sharpe AH, Freeman GJ, and Oldstone MB. 2008 'IL-10 and PD-L1 operate through distinct pathways to suppress T-cell activity during persistent viral infection', Proc Natl Acad Sci U S A, 105: 20428–33. [PubMed: 19075244]

Chen G, Huang AC, Zhang W, Zhang G, Wu M, Xu W, Yu Z, et al. 2018 'Exosomal PD-L1 contributes to immunosuppression and is associated with anti-PD-1 response', Nature, 560: 382–86. [PubMed: 30089911]

Ellerhorst JA, Greene VR, Ekmekcioglu S, Warneke CL, Johnson MM, Cooke CP, Wang LE, et al. 2011 'Clinical correlates of NRAS and BRAF mutations in primary human melanoma', Clin Cancer Res, 17: 229–35. [PubMed: 20975100]

Emmerich J, Mumm JB, Chan IH, LaFace D, Truong H, McClanahan T, Gorman DM, and Oft M. 2012 'IL-10 directly activates and expands tumor-resident CD8(+) T cells without de novo infiltration from secondary lymphoid organs', Cancer Res, 72: 3570–81. [PubMed: 22581824]

Feng D, Qin B, Pal K, Sun L, Dutta S, Dong H, Liu X, Mukhopadhyay D, Huang S, and Sinicrope FA. 2019 'BRAF(V600E)-induced, tumor intrinsic PD-L1 can regulate chemotherapy-induced apoptosis in human colon cancer cells and in tumor xenografts', Oncogene, 38: 6752–66. [PubMed: 31406255]

Garcia-Silva S, Benito-Martin A, Sanchez-Redondo S, Hernandez-Barranco A, Ximenez-Embun P, Nogues L, Mazariegos MS, et al. 2019 'Use of extracellular vesicles from lymphatic drainage as surrogate markers of melanoma progression and BRAF (V600E) mutation', J Exp Med, 216: 1061–70. [PubMed: 30975894]

Ikeda H, Old LJ, and Schreiber RD. 2002 'The roles of IFN gamma in protection against tumor development and cancer immunoediting', Cytokine Growth Factor Rev, 13: 95–109. [PubMed: 11900986]

Ilieva KM, Correa I, Josephs DH, Karagiannis P, Egbuniwe IU, Cafferkey MJ, Spicer JF, et al. 2014 'Effects of BRAF mutations and BRAF inhibition on immune responses to melanoma', Mol Cancer Ther, 13: 2769–83. [PubMed: 25385327]

Kasahara T, Hooks JJ, Dougherty SF, and Oppenheim JJ. 1983 'Interleukin 2-mediated immune interferon (IFN-gamma) production by human T cells and T cell subsets', J Immunol, 130: 1784–9. [PubMed: 6403613]

Kelleher RJ Jr., Balu-Iyer S, Loyall J, Sacca AJ, Shenoy GN, Peng P, Iyer V, et al. 2015 'Extracellular Vesicles Present in Human Ovarian Tumor Microenvironments Induce a Phosphatidylserine-

Dependent Arrest in the T-cell Signaling Cascade', Cancer Immunol Res, 3: 1269–78. [PubMed: 26112921]

Keller S, Konig AK, Marme F, Runz S, Wolterink S, Koensgen D, Mustea A, Sehouli J, and Altevogt P. 2009 'Systemic presence and tumor-growth promoting effect of ovarian carcinoma released exosomes', Cancer Lett, 278: 73–81. [PubMed: 19188015]

Khalili JS, Liu S, Rodriguez-Cruz TG, Whittington M, Wardell S, Liu C, Zhang M, et al. 2012 'Oncogenic BRAF(V600E) promotes stromal cell-mediated immunosuppression via induction of interleukin-1 in melanoma', Clin Cancer Res, 18: 5329–40. [PubMed: 22850568]

Liu S, Matsuzaki J, Wei L, Tsuji T, Battaglia S, Hu Q, Cortes E, et al. 2019 'Efficient identification of neoantigen-specific T-cell responses in advanced human ovarian cancer', J Immunother Cancer, 7: 156. [PubMed: 31221207]

Lorre K, Fransen L, and Ceuppens JL. 1992 'Interleukin-2 induces tumor necrosis factor-alpha production by activated human T cells via a cyclosporin-sensitive pathway', Eur Cytokine Netw, 3: 321–30. [PubMed: 1353987]

Marleau AM, Chen CS, Joyce JA, and Tullis RH. 2012 'Exosome removal as a therapeutic adjuvant in cancer', J Transl Med, 10: 134. [PubMed: 22738135]

Matsumura S, Minamisawa T, Suga K, Kishita H, Akagi T, Ichiki T, Ichikawa Y, and Shiba K. 2019 'Subtypes of tumour cell-derived small extracellular vesicles having differently externalized phosphatidylserine', J Extracell Vesicles, 8: 1579541. [PubMed: 30834072]

Matsuzaki J, Gnjatic S, Mhawech-Fauceglia P, Beck A, Miller A, Tsuji T, Eppolito C, et al. 2010 'Tumor-infiltrating NY-ESO-1-specific CD8+ T cells are negatively regulated by LAG-3 and PD-1 in human ovarian cancer', Proc Natl Acad Sci U S A, 107: 7875–80. [PubMed: 20385810]

Matsuzaki J, Tsuji T, Luescher IF, Shiku H, Mineno J, Okamoto S, Old LJ, Shrikant P, Gnjatic S, and Odunsi K. 2015 'Direct tumor recognition by a human CD4(+) T-cell subset potently mediates tumor growth inhibition and orchestrates anti-tumor immune responses', Sci Rep, 5: 14896. [PubMed: 26447332]

Maybruck BT, Pfannenstiel LW, Diaz-Montero M, and Gastman BR. 2017 'Tumor-derived exosomes induce CD8(+) T cell suppressors', J Immunother Cancer, 5: 65. [PubMed: 28806909]

Mortara L, Balza E, Sassi F, Castellani P, Carnemolla B, De Lerma Barbaro A, Fossati S, Tosi G, Accolla RS, and Borsi L. 2007 'Therapy-induced antitumor vaccination by targeting tumor necrosis factor alpha to tumor vessels in combination with melphalan', Eur J Immunol, 37: 3381–92. [PubMed: 18022863]

Mumm JB, Emmerich J, Zhang X, Chan I, Wu L, Mauze S, Blaisdell S, et al. 2011 'IL-10 elicits IFNgamma-dependent tumor immune surveillance', Cancer Cell, 20: 781–96. [PubMed: 22172723]

Roato I, Brunetti G, Gorassini E, Grano M, Colucci S, Bonello L, Buffoni L, et al. 2006 'IL-7 up-regulates TNF-alpha-dependent osteoclastogenesis in patients affected by solid tumor', PLoS One, 1: e124. [PubMed: 17205128]

Robert C, Schachter J, Long GV, Arance A, Grob JJ, Mortier L, Daud A, et al. 2015 'Pembrolizumab versus Ipilimumab in Advanced Melanoma', N Engl J Med, 372: 2521–32. [PubMed: 25891173]

Russell AE, Sneider A, Witwer KW, Bergese P, Bhattacharyya SN, Cocks A, Cocucci E, et al. 2019 'Biological membranes in EV biogenesis, stability, uptake, and cargo transfer: an ISEV position paper arising from the ISEV membranes and EVs workshop', J Extracell Vesicles, 8: 1684862. [PubMed: 31762963]

Sa G, Das T, Moon C, Hilston CM, Rayman PA, Rini BI, Tannenbaum CS, and Finke JH. 2009 'GD3, an overexpressed tumor-derived ganglioside, mediates the apoptosis of activated but not resting T cells', Cancer Res, 69: 3095–104. [PubMed: 19276353]

Shabaneh TB, Molodtsov AK, Steinberg SM, Zhang P, Torres GM, Mohamed GA, Boni A, Curiel TJ, Angeles CV, and Turk MJ. 2018 'Oncogenic BRAF(V600E) Governs Regulatory T-cell Recruitment during Melanoma Tumorigenesis', Cancer Res, 78: 5038–49. [PubMed: 30026331]

Sharma P, Diergaarde B, Ferrone S, Kirkwood JM, and Whiteside TL. 2020 'Melanoma cell-derived exosomes in plasma of melanoma patients suppress functions of immune effector cells', Sci Rep, 10: 92. [PubMed: 31919420]

Shenoy GN, Loyall J, Berenson CS, Kelleher RJ Jr., Iyer V, Balu-Iyer SV, Odunsi K, and Bankert RB. 2018 'Sialic Acid-Dependent Inhibition of T Cells by Exosomal Ganglioside GD3 in Ovarian Tumor Microenvironments', J Immunol, 201: 3750–58. [PubMed: 30446565]

Shenoy GN, Loyall J, Maguire O, Iyer V, Kelleher RJ Jr., Minderman H, Wallace PK, Odunsi K, Balu-Iyer SV, and Bankert RB. 2018 'Exosomes Associated with Human Ovarian Tumors Harbor a Reversible Checkpoint of T-cell Responses', Cancer Immunol Res, 6: 236–47. [PubMed: 29301753]

Shu S, Yang Y, Allen CL, Hurley E, Tung KH, Minderman H, Wu Y, and Ernstoff MS. 2020 'Purity and yield of melanoma exosomes are dependent on isolation method', J Extracell Vesicles, 9: 1692401. [PubMed: 31807236]

Shu S, Yang Y, Allen CL, Maguire O, Minderman H, Sen A, Ciesielski MJ, et al. 2018 'Metabolic reprogramming of stromal fibroblasts by melanoma exosome microRNA favours a pre-metastatic microenvironment', Sci Rep, 8: 12905. [PubMed: 30150674]

Sumimoto H, Imabayashi F, Iwata T, and Kawakami Y. 2006 'The BRAF-MAPK signaling pathway is essential for cancer-immune evasion in human melanoma cells', J Exp Med, 203: 1651–6. [PubMed: 16801397]

Sun Z, Fourcade J, Pagliano O, Chauvin JM, Sander C, Kirkwood JM, and Zarour HM. 2015 'IL10 and PD-1 Cooperate to Limit the Activity of Tumor-Specific CD8+ T Cells', Cancer Res, 75: 1635–44. [PubMed: 25720800]

Tung KH, Ernstoff MS, Allen C, and Shu S. 2019 'A Review of Exosomes and their Role in The Tumor Microenvironment and Host-Tumor "Macroenvironment"', J Immunol Sci, 3: 4–8. [PubMed: 30972385]

Whipple CA, Boni A, Fisher JL, Hampton TH, Tsongalis GJ, Mellinger DL, Yan S, et al. 2016 'The mitogen-activated protein kinase pathway plays a critical role in regulating immunological properties of BRAF mutant cutaneous melanoma cells', Melanoma Res, 26: 223–35. [PubMed: 26974965]

Whiteside TL. 2016 'Tumor-Derived Exosomes and Their Role in Tumor-Induced Immune Suppression', Vaccines (Basel), 4.

Whiteside TL. 2018 'The potential of tumor-derived exosomes for noninvasive cancer monitoring: an update', Expert Rev Mol Diagn, 18: 1029–40. [PubMed: 30406709]

Zhang HG, and Grizzle WE. 2011 'Exosomes and cancer: a newly described pathway of immune suppression', Clin Cancer Res, 17: 959–64. [PubMed: 21224375]

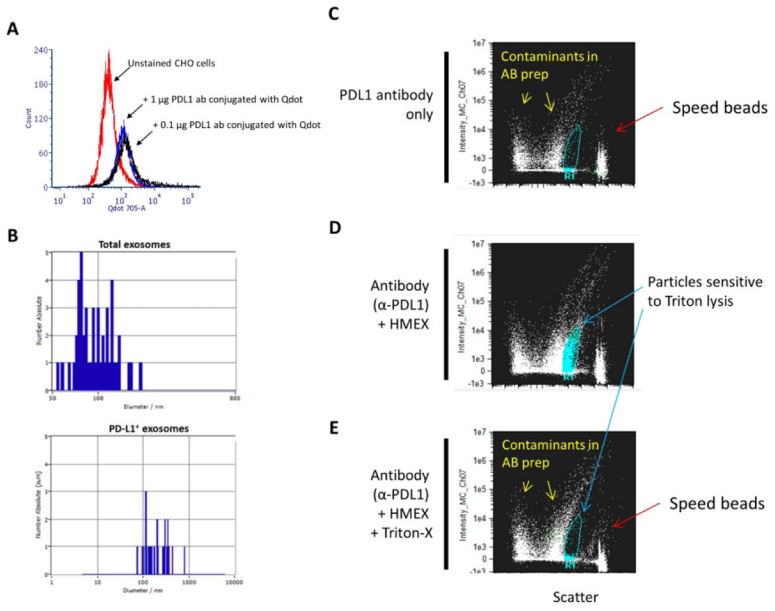

Figure 1.

Detection of PD-L1 on HMEX A) Confirmation of successful conjugation of PD-L1 to Qdot 705 using SiteClick and post-purification process. Flow cytometry histogram of untreated PD-L1(+) CHO cells were used to set baseline for background/non-fluorescent signal, with positive signal determined by incubating 0.1 µg or 1 µg of conjugated PD-L1 Qdot 705 antibody with PD-L1(+) CHO cells. There is no observable difference in mean fluorescent intensity (MFI) between the two concentrations, indicating that 0.1 µg of antibody is a sufficient saturating concentration for detection of PD-L1 positive cells. B) Detection of a subpopulation of exosomes using fluorescent NTA. Total exosome number was measured using NTA. This was followed by fluorescent NTA with 688 +/− 20 nm bypass filter for detection of Qdot 705 conjugated PD-L1 antibody incubated exosomes. C–E) PD-L1 positive exosomes are membrane-bound vesicles that can be detected by ImageStream. This population is not detected upon treatment with a strong detergent (Triton-X). C) At the highest sensitivity settings, speed beads (~ 1 µm in size) are detected at the rightmost axis with a low scatter particulate banding pattern that is present when antibody, in absence of exosomes, is examined, indicating particulate contaminant patterns due to presence of antibodies. D) Detection of positive signal with intermediate scatter intensity indicative of PD-L1 positive exosomes. A distinct clustering of particulates is detected and present when PD-L1 antibody was co-incubated with exosomes. E) Loss of PD-L1 positive cluster of particulates upon addition of strong detergent (Triton-X), indicating that the clustered particles are membranous vesicles.

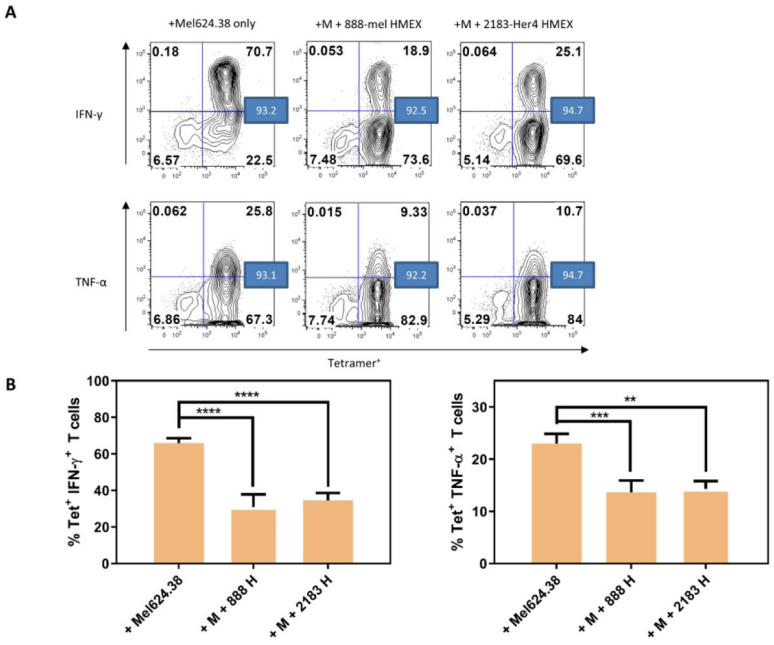

Figure 2.

HMEX are inhibitory to NY-T cell IFN-γ and TNF-α positive populations. For consistency, HMEX used (888-mel or 2183-Her4) were matched for exosome number based on NTA data (1.0×10^{10} per well/sample). A) Flow cytometry analysis of NY-T cells co-incubated with Mel624.38 (+Mel624.38 only, M); NY-T cells and Mel624.38 with 888-mel HMEX (+M +888-mel HMEX); and NY-T cells and Mel624.38 with 2183-Her4 HMEX (+M +2183-Her4 HMEX) for IFN-γ and TNF-α. The values in the blue boxes represent percentage of tetramer positive cells. Histograms are derived from one experiment. B) Graphical representation of samples shown in A) (n=3).

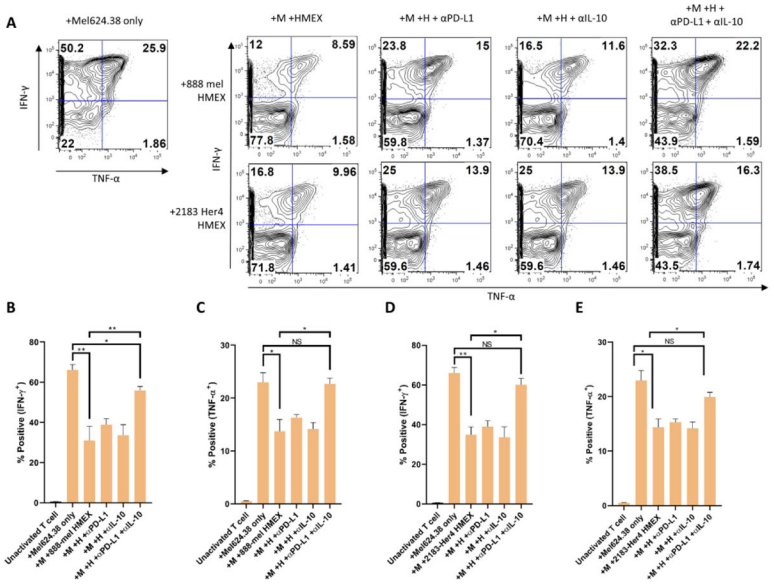

Figure 3.

Suppression of NY-T cell activity by HMEX can be restored using a combination of PD-L1 and IL-10 neutralizing antibodies. Cells were pre-gated on $CD8^+$ and tetramer $(NY\text{-}ESO\text{-}1)^+$ populations. For consistency, HMEX used (888-mel or 2183-Her4) were matched for exosome number based on NTA data (1.0×10^{10} per well/sample). A) Flow cytometry analysis of IFN-γ and TNF-α positive populations in NY-T cells co-incubated with Mel624.38 and either 888-mel or 2183-Her4 HMEX that were pre-incubated in the presence or absence of PD-L1 and IL-10 neutralizing antibodies (in combination, or separately). The decrease in the percentage of cytokine-positive NY-T cells resulting from culture with HMEX was restored to a greater extent when HMEX were incubated in the presence of both PD-L1 and IL-10 neutralizing Ab's than in the presence of the neutralizing antibodies separately. Histograms are derived from one experiment. NY-T cells co-incubated with Mel624.38 (+Mel624.38 only, M); NY-T cells co-incubated with Mel624.38 and HMEX (+M +HMEX); NY-T cells co-incubated with Mel624.38 and HMEX with αPD-L1 (+M +H + αPD-L1); NY-T cells co-incubated with Mel624.38 and HMEX with αIL-10 (+M +H + αIL-10); NY-T cells co-incubated with Mel624.38 and HMEX with both neutralizing Ab's (+M +H + αPD-L1+ αIL-10). B) Graphical representation of samples shown in A (n=3). Unactivated T cell: NY-T cells alone.